Lightweight and Anisotropic Porous MWCNT/WPU Composites for Ultrahigh Performance Electromagnetic Interference Shielding

Zhihui Zeng, Hao Jin, Mingji Chen, Weiwei Li, Licheng Zhou, and Zhong Zhang**

Lightweight, flexible and anisotropic porous multiwalled carbon nanotube (MWCNT)/water-borne polyurethane (WPU) composites are assembled by a facile freeze-drying method. The composites contain extremely wide range of MWCNT mass ratios and show giant electromagnetic interference (EMI) shielding effectiveness (SE) which exceeds 50 or 20 dB in the X-band while the density is merely 126 or 20 mg cm^{-3}, respectively. The relevant specific SE is up to 1148 dB cm^3 g^{-1}, greater than those of other shielding materials ever reported. The ultrahigh EMI shielding performance is attributed to the conductivity of the cell walls caused by MWCNT content, the anisotropic porous structures, and the polarization between MWCNT and WPU matrix. In addition to the enhanced electrical properties, the composites also indicate enhanced mechanical properties compared with porous WPU and CNT architectures.

1. Introduction

High-performance electromagnetic interference (EMI) shielding materials are essential to address the problems of electromagnetic wave attenuation in both civil and military applications.[1–4] Compared to traditional metal-based shielding materials, which suffer from high mass density, poor flexibility, undesirable corrosion susceptibility, and limited tuning of shielding effectiveness (SE), conductive polymer composites (CPCs) have attracted numerous researchers due to the advantages in mass density, shaping capability, chemical stability, and design flexibility.[5–7] Especially, effective reduction of weight and efficient utilization of energy and materials are crucial to some practical EMI shielding applications such as in areas of aircraft, spacecraft, or portable electronics.[8–10]

Z. Zeng, Dr. H. Jin, Dr. M. Chen, W. Li, Prof. Z. Zhang
CAS Key Laboratory of Nanosystem and Hierarchical Fabrication
National Center for Nanoscience and Technology
Beijing 100190, P.R. China
E-mail: hjin@nanoctr.cn; zhong.zhang@nanoctr.cn
Z. Zeng, W. Li
University of Chinese Academy of Sciences
Beijing 100049, P.R. China
L. Zhou
State Key Laboratory for Turbulence and Complex Systems
College of Engineering
Peking University
Beijing 100871, P.R. China

DOI: 10.1002/adfm.201503579

EMI SE reveals the ability of materials to attenuate electromagnetic waves and is generally expressed in decibel (dB).[11,12] For the applications that need lightweight shielding materials, however, the specific SE (SSE), which is defined as SE divided by mass density, is also a crucial criterion.[8] In porous CPCs, the air bubbles arise in the material and thus the mass density is reduced. If conductive networks are formed therein by the electric fillers with large aspect ratios, such as carbon fibers (CFs), carbon nanotubes (CNTs), or graphene layers, it will lead to high electrical conductivity in addition to the low density,[9,13,14] which are beneficial to high-efficiency EMI shielding.[10,15–20] In consideration of that, Yang et al. reported porous CPC-based EMI shielding material of 15 wt% carbon nanofiber/polystyrene (PS) composite foams with SE ≈19 dB in the frequency range of 8.2–12.4 GHz (X-band),[16] and 7 wt% CNT/PS porous composite fabricated with the aid of chemical blowing agents obtained SE ≈19 dB at a density of 0.56 g cm^{-3}.[17] Those porous CPCs indicate higher utilization of materials than typical metal-based shields, as SSE is 33.1 dB cm^3 g^{-1} for 7 wt% CNT/PS composite foams[17] and 16–25 dB cm^3 g^{-1} for 5 wt% porous graphene/polymethylmethacrylate (PMMA) composites,[18] higher than that of solid copper ≈10 dB cm^3 g^{-1}.[21] To obtain higher SSE, various preparation methods of CPC-based foams are developed to further decrease the density or improve the SE at similar thickness. Zheng group[20] reported a facile phase separation method to fabricate lightweight microcellular graphene/polyetherimide (PEI) and graphene@Fe_3O_4/PEI composites with density near 0.3 g cm^{-3} and SSE ≈40 dB cm^3 g^{-1} at 2.3–2.5 mm thickness. Yan et al. fabricated porous graphene/PS composites with density of 0.27 and 0.45 g cm^{-3} by a combination of high-pressure compression molding and salt-leaching method, and the SSE was as large as 64.4 dB cm^3 g^{-1} in the X-band at 2.5 mm thickness, due to successful preparation of low-density porous composites with the loading of graphene as high as 30 wt%.[10] However, SE of those porous composites are still not high enough when the densities are relatively low, and SSE of those CPC-based foams are limited at similar thickness.

For a certain thickness, improving the conductivities of CPCs is an effective way to improve SE by increasing the loadings of electric fillers with high conductivity. Nevertheless, the conductive network in the matrix will inevitably be impaired in the foaming process and results in a lower conductivity

compared to solid composites,[18–20] a high-conductivity filler loading of CPC-based foam or porous architecture with low density and superior EMI SE is still a daunting challenge.[10,19] Moreover, even though the porous architectures are considered to be instrumental in improving the SE by introducing interfaces between cell walls and pores to enhance the multireflection of the incident waves,[5,16,19,20] an efficient utilization of the existing pores is still insufficient due to the difficulty in control of the porous shapes with those preparation methods.

Freeze-drying method as a simple and efficient approach to fabricate 3D highly porous monoliths can endow materials with low densities and high specific surfaces,[22] and as a template-free preparation method it is desirable for scalable manufacturing of aerogels with controllable densities and shapes.[23] In this paper, aqueous solutions of multiwalled carbon nanotube (MWCNT) and water-borne polyurethane (WPU) are utilized to assemble a type of CPC-based anisotropic or aligned porous composites with low and controllable densities by an unidirectional freeze-drying process (Figure S1, Supporting Information). The manufactured MWCNT/WPU porous composites possess wide range of electric MWCNT filler loading, attributed to the combination of dispersion and pore forming methods, which is superior to that of other porous shielding materials previously reported. High conductive filler loading of CPC-based highly porous foams with low density makes it promising as high-performance shielding materials with superior SE and SSE. More importantly, anisotropic porous structure can be obtained in the composites and is in favor of the comparison of EMI shielding performance among different porous orientations, which is instructive in optimizing EMI SE caused by porous shapes.

2. Results and Discussion

Herein, noncovalently functionalized[24] MWCNT dispersion, and WPU emulsion, which have the advantages of nontoxicity, nonflammability, nonvolatility and available application of polyurethane with good flexibility in an aqueous medium,[25] are mixed and poured into designed mould followed by freeze-drying process to get the porous composites with various shapes or sizes (**Figure 1**a). The freezing method resulted from large temperature gradient between the bottom and top of the MWCNT/WPU mixed solution is adopted and leads to the formation and unidirectional growth of ice crystals from the bottom to upper face (Figure S1c, Supporting Information). The growing ice crystals exclude the particles from the freezing front, leading to the formation of MWCNT/WPU composite cell walls. The porous architectures with aligned pores that are templated from the spaces occupied by the ice crystals[22] are obtained by sublimating the ice of the hydrogel in the freeze-drying process. Large-area and lightweight porous composites with various densities can also be prepared and indicate excellent flexibility (Figure 1b–d and Figure S2a–h, Supporting

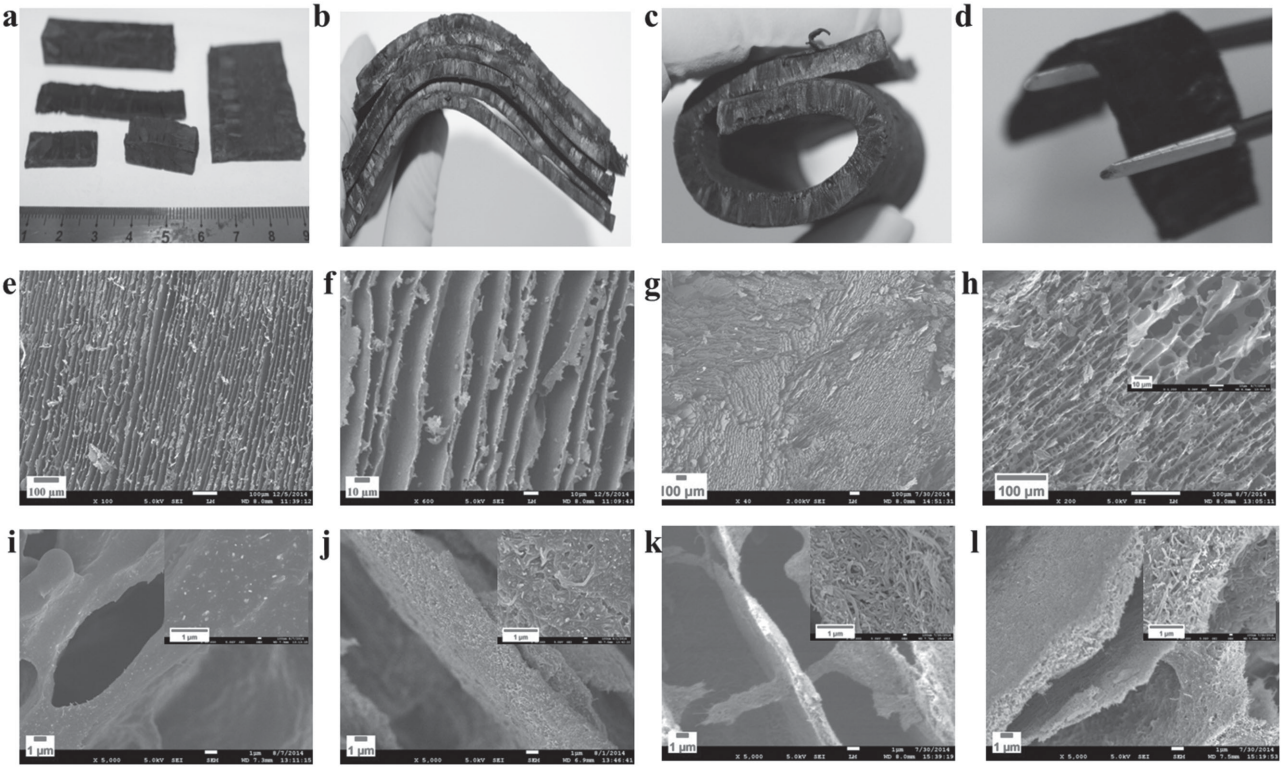

Figure 1. a) Optical images of porous MWCNT/WPU composites with various shapes. Flexible performance of 76.2 wt% porous MWCNT/WPU composites with various densities: b) (down to up) 126, 95, 71, 39, 30, and 20, c) 70, and d) 20 mg cm^{-3}. SEM images in (e,f) through-plane and (g,h) in-plane of the anisotropic porous structure of the composites (scale bar is 10 μm for inset image in (h)). Cell-wall structures of the anisotropic porous composites with various MWCNT contents: i) 28.6 wt%, j) 50.0 wt%, k) 66.7 wt%, and l) 76.2 wt% (scale bar is 1 μm for inset image in (i–l)).

Information). The MWCNT/WPU composites indicate anisotropic porous microstructure in the scale of micrometers (Figure 1e–h), compared with the WPU foam that is contraction state because of bulking instability attributed to the low mechanical modulus of WPU film (Figure S2i,j, Supporting Information). The anisotropic porous architectures interconnect by cell walls which are composed of the MWCNT/WPU composite films. Attributed to the pore forming mechanism, cell walls of the porous composites are randomly oriented in in-plane direction (perpendicular to the growth direction of ice), thus the foam structure tends to be isotropic in this direction. While due to the assembly of MWCNT/WPU composites as cell walls via the unidirectional growth of ice crystals in the freezing process, the porous architectures indicate the anisotropic structures in through-plane direction (Figure 1e,f). In the cell walls, MWCNTs are dispersed as enhanced nanofillers in WPU matrix but bonded by WPU matrix at higher MWCNT loading of composites (Figure 1i–l).

Compression experiments on the anisotropic porous MWCNT/WPU composites also imply the structure. Through-plane strength and modulus of MWCNT/WPU composites are higher than the in-plane ones, respectively, due to more cell walls along through-plane direction of the composites (**Figure 2** and Table S1, Supporting Information). The modulus indicates an increasing behavior with increasing MWCNT contents first, e.g., through-plane modulus of 28.6, 50, and 66.7 wt% MWCNT/WPU composite foams are 466, 510, and 2224 kPa, respectively, and are 288%, 325%, and 1753% higher, respectively, than that of pure WPU foam (≈120 kPa); however, modulus of the composites with higher MWCNT contents do not continue to increase drastically but decrease. The 76.2 wt% MWCNT/WPU composites and MWCNT foams have through-plane modulus 1222 and 191 kPa, respectively. It is accessible that more effective interfaces between rigid fillers and polymer matrix are instrumental in higher modulus of composite;[26] however, too high MWCNT mass ratios correspond to less effective interfaces, which may reduce the compressive modulus of the porous composites. Therefore, MWCNT foams at similar densities without WPU as binders or supporting matrix indicate much lower modulus than the porous MWCNT/WPU composites.

EMI SE of the anisotropic porous MWCNT/WPU composite is measured first when direction of wave propagation is parallel to the in-plane direction of the sample. SE of the porous MWCNT/WPU composites is almost independent on the frequency, which increases with increasing MWCNT mass ratios and conductivities (**Figure 3**a). 76.2 wt% MWCNT/WPU foams with density of 126 mg cm^{-3} indicate EMI SE ≈52 dB in the whole X-band frequency range, much higher than other typical porous CPCs at similar thickness ever reported (13–19 dB for 5.0 wt% graphene/PMMA foams at 2.4 mm and 790 mg cm^{-3},[18] ≈29 dB for 30 wt% graphene/PS foam at 2.5 mm and 450 mg cm^{-3},[10] or 24.9 dB for 10 vol% CF/polypropylene (PP) foam at 3.1 mm and 740 mg cm^{-3}.[19]) Such high SE of our porous composites may be mainly attributed to the successful preparation of CPC-based foams with high electrically conductive MWCNT mass ratio and high conductivity of cell walls (Table S2, Supporting Information). The 66.7 wt% MWCNT/WPU foams with density of 136 mg cm^{-3} also show SE of 48.4 dB almost corresponding to 0.001% transmission of electromagnetic waves from the shields.

It is worth noting that the volume fraction of nanofillers in the porous composites is low (Table S2, Supporting Information), as 76.2 and 28.6 wt% MWCNT contents are equivalent only to 7.2 and 4.4 vol% MWCNT volume contents in the foams, and thus our 4.4 vol% MWCNT/WPU porous composites satisfy SE requirement of 20 dB for practical EMI shielding applications.[11,12] In addition, the MWCNT/WPU foams with 50.0 wt% MWCNT content also indicate conductivity and SE higher than MWCNT foams at similar densities (Figure 3a), which is similar to the performance of compressive modulus. This may be ascribed to role of WPU in the cell walls of the porous composites plays as a type of organic binder that promote a better connection of MWCNTs to reduce the contact resistance and improve the channels for the mobile carrier's movement, and the interfacial polarization originating from the interaction between MWCNT and WPU can also lead to the increase of SE.[3,7,27]

One advantage of the preparation method in this work is that the density of porous materials can be controlled by adjusting the solvent amount and here the water fraction of MWCNT/WPU mixed solutions. The porous MWCNT/WPU composites with various densities are effortlessly prepared by controlling the water fraction before mixed solutions are frozen. Higher water content corresponds to higher porosity (calculation is shown in the Supporting Information) and lower density of prepared MWCNT/WPU foams (Figure 3b). The 76.2 wt% MWCNT/WPU foams with density ranging from

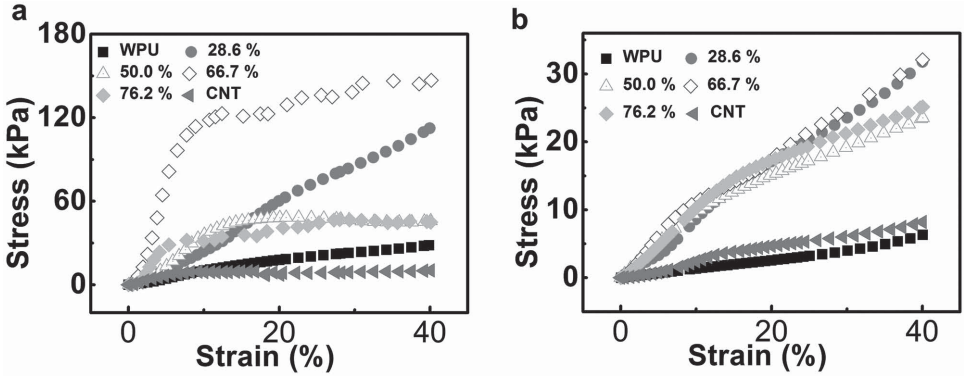

Figure 2. Compressive tests of porous materials with various MWCNT mass ratios along a) through-plane and b) in-plane direction.

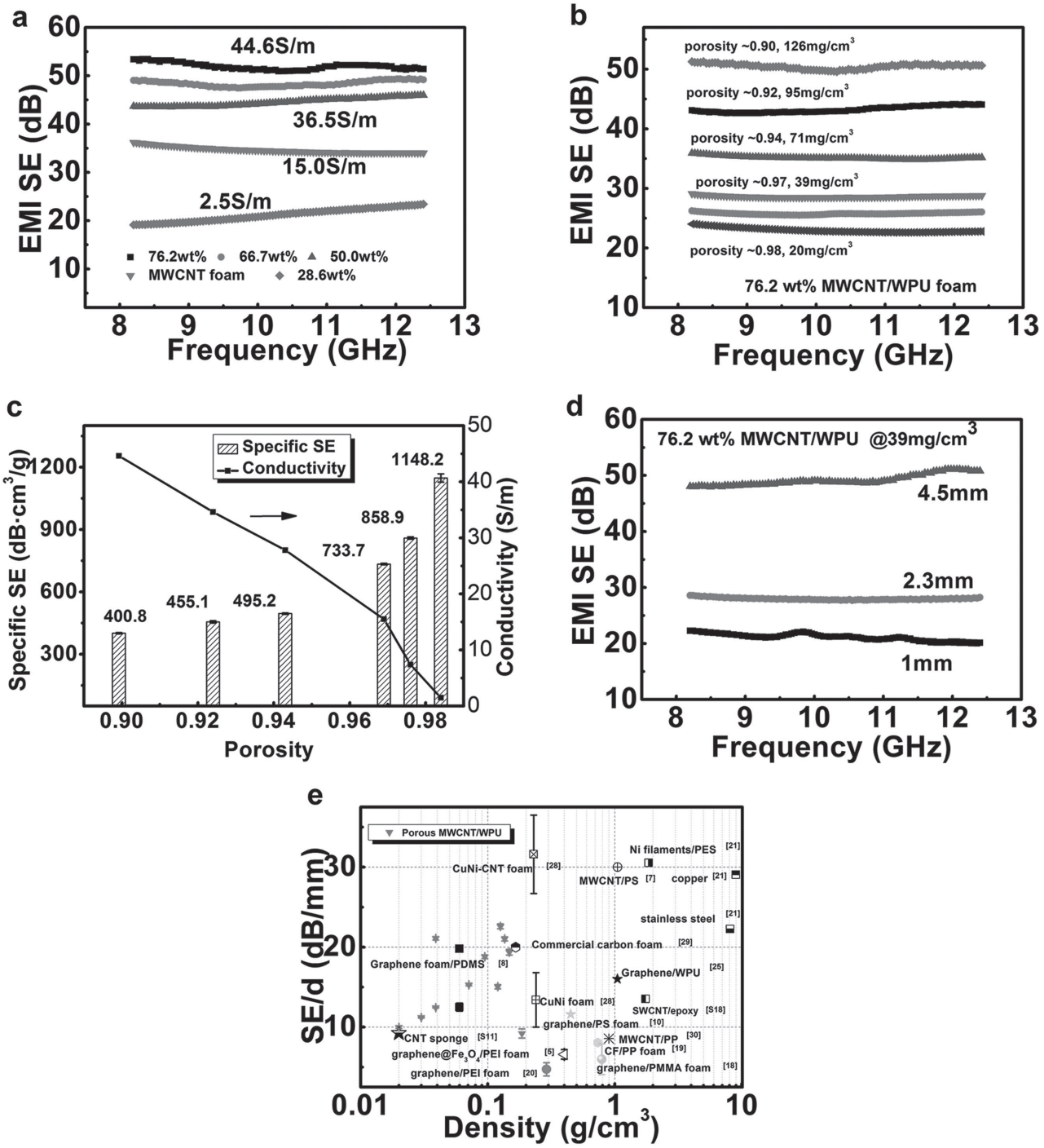

Figure 3. a) EMI SE in the X-band of porous composites with various MWCNT contents, b) EMI SE of 76.2 wt% MWCNT/WPU foams with various densities, c) specific SE in the whole X-band and conductivity of 76.2 wt% MWCNT/WPU foams as a function of porosity, d) EMI SE in the X-band of 76.2 wt% MWCNT/WPU foams with density of 39 mg cm^{-3} at various thicknesses, and e) comparison of shielding performance of the shielding materials ever reported in terms of that SE divided by thickness as a function of density (EMI SE in the X-band except copper, nickel, and Ni filaments/polyethersulfone with SE at 1–2 GHz).

20 to 126 mg cm^{-3} show porosity and SE greater than 90% and 23 dB, respectively. The controllable densities mean devisable weight reduction of our porous composites, as it indicates 98.4 wt% reduction of weight for 76.2 wt% MWCNT/WPU foams at 20 mg cm^{-3} (Table S3, Supporting Information).

SE and electrical conductivities of the porous MWCNT/WPU composites decrease with increasing porosity (or decreasing density), while the SSE shows an increasing behavior (Figure 3b,c). High MWCNT mass ratio in the cell walls of the porous composites may ensure the integrity of the MWCNT

conductive networks in comparison with low MWCNT mass ratio of CPC-based foams that show significant percolation phenomenon with decreasing density,[9] thus SE and electrical conductivity of our 76.2 wt% MWCNT/WPU foams do not decrease much with drastically decreasing density and the SSE increases with increasing porosity. More importantly, the SSE (1148 dB cm^3 g^{-1} in the X-band) of our anisotropic porous MWCNT/WPU composites is much higher than those of other shielding materials at similar thickness (Table S4, Supporting Information) including typical metal or alloy-based porous materials (10 and ≈9 dB cm^3 g^{-1} for solid copper and nickel, respectively,[21] 174–237 dB cm^3 g^{-1} for Cu-Ni-CNT foams,[28] porous CPCs (33.1 dB cm^3 g^{-1} for 7 wt% CNT/PS foams,[17] 64.4 dB cm^3 g^{-1} for 30 wt% graphene/PS foam at 2.5 mm[10] and 400–467 dB cm^3 g^{-1} for graphene foam-based polydimethylsiloxane composites at 2 mm[8] and commercial carbon foam (241 dB cm^3 g^{-1} at 2 mm thickness.[29] The high SSE of our porous MWCNT/WPU composites, combining with the controllable manufacturing of various densities of foams that means the devisable SSE, indicates the great potentials for various EMI shielding applications as lightweight and high-performance shielding materials.

Our 76.2 wt% MWCNT/WPU foams with density of 39 mg cm^{-3}, corresponding to only 2.2 vol% MWCNT content, are also prepared at various thicknesses and the SE increases with increasing thickness (Figure 3d) because of increasing amount of conductive MWCNT fillers interacting with the electromagnetic fields.[3,11] The 2.2 vol% MWCNT/WPU foams show SE from 21.1 to 49.2 dB at thickness ranging from 1 to 4.5 mm. EMI SE in the X-band of our composites (≈28.0 dB for MWCNT/WPU foams containing 2.2 vol% MWCNTs at 2.3 mm thickness (Table S3, Supporting Information)) is higher than those of most typical carbon-based CPCs at similar volume content and thickness (24 dB for 5 vol% MWCNT/PP composites at 2.8 mm thickness,[30] 9–12.8 dB for 5.87 vol% graphene/PEI foams at 2.3 mm thickness[20] (Table S4, Supporting Information). The SSE of our MWCNT/WPU foams with SE greater than 20 dB in the whole X-band can reach as large as 541 dB cm^3 g^{-1} at 1 mm thickness, which also shows the highest value in comparison with other shielding materials at that thickness. That EMI SE divided by thickness of the shielding materials as a function of density is obtained in order to more clearly realize the EMI shielding performance (Figure 3e). Those typical porous architectures, solid CPCs, and metal-based shields are compared in terms of the EMI SE, thickness, and density, which indicate various density ranges obviously. Our porous MWCNT/WPU composites can obtain wide ranges of density and EMI SE, and more importantly, the largest normalized value in terms of EMI SE divided by the thickness and density are distinct observed and calculated as 5410 dB cm^2 g^{-1}, compared with those of other shielding materials ever reported (Table S4, Supporting Information).

EMI shielding is under the influence of three major mechanisms as reflection, absorption, and multiple reflections, which are mainly related to mobile charge carriers, electric (or magnetic) dipoles, and reflections at various surfaces or interfaces, respectively.[3] The total SE (SE_T) consists of the contributions from reflection (SE_R), absorption (SE_A), and multiple reflections (SE_{MR}). To analyze the ultrahigh EMI shielding performance of our porous MWCNT/WPU composites, the SE_T, SE_A, and SE_R of 66.7 wt% MWCNT/WPU foams with the best mechanical performance at various densities are shown as a function of MWCNT volume contents at 10 GHz (**Figure 4**a and Table S5, Supporting Information). It can be seen that SE_T and SE_A increase with increasing MWCNT volume contents while SE_R increases slightly and SE_A dominates as high as ≈80% of the total shielding. The MWCNT amount or volume content decreases obviously with decreasing density of the foams and leads to decrease of SE_A (or SE_T) with decreasing charge carriers and dipole amount.[7,27] However, attributed to the same freezing way and condition to the mixed solution as discussed above, the conductive MWCNT networks in the cell walls are indeed still intact, and the average distance (gap) between adjacent cell walls can keep similar that is beneficial to the reservation of enough interfaces between cell walls and the pores in in-plane direction for those high MWCNT content of porous composites, even though the thickness and size of cell walls decrease much as the density decreases by as low as 29 mg cm^{-3} (Figure 4b–d, and Figure S3 and Table S6, Supporting Information). As a result, the conductivity and SE of our high MWCNT mass ratio of foams do not show sharp decrease with dramatically decreasing density and hence the SSE increases. Furthermore, through-plane SE_T (T-SE_T), SE_A (T-SE_A), and SE_R (T-SE_R) of the porous MWCNT/WPU composites at 2.3 mm thickness are obtained, indicating the shielding performance of the samples when the electromagnetic waves pass along this direction, in which the unidirectional growth of ice takes place as well. The quantity of cell walls in this direction is significantly less than that in the perpendicular (in-plane) direction due to the cell wall structures of composite MWCNT/WPU formed on the surface of ice crystals. Considering the similar conductivity in both directions (Table S2, Supporting Information), the theoretically calculated (shown in the Supporting Information) SE_T (M-SE_T), SE_A (M-SE_A), and SE_R (M-SE_R) based only on conductivity factor (electric or ohmic loss) are compared (Figure 4e and Figure S4, Supporting Information). In fact, the interfacial polarization between conductive MWCNT and WPU matrix improves the polarization loss of the MWCNT/WPU composite cell walls to the incident wave, and thus the SE_A of the composite. It can be seen that those SE_R values almost keep no different due to the impact of conductivity, while slightly lower M-SE_T (or M-SE_A) than T-SE_T (or T-SE_A) at relatively low conductivity. Combining with the discussion in the calculation section (shown in the Supporting Information), the comparison of M-SE_A and T-SE_A in the relatively low conductivity range for the porous composites (as shown in Table S5, Supporting Information) implies the nonignorable polarization effect on the SE in the porous composites.[1,3] And that the theoretical calculated shielding performance is close to through-plane performance of the porous composites for higher conductivity range can indicate dominant influence of the conductivity. However, the SE_T (or SE_A) that indicates the in-plane shielding performance can reveal much greater value than through-plane values and theoretical predictions. Actually, the incorporation of air bubbles not only reduces the weight of CPCs but also can alter some electrical or electromagnetic parameters such as decreasing percolation threshold[14] or dielectric constant,[31] introducing more interfaces that improve

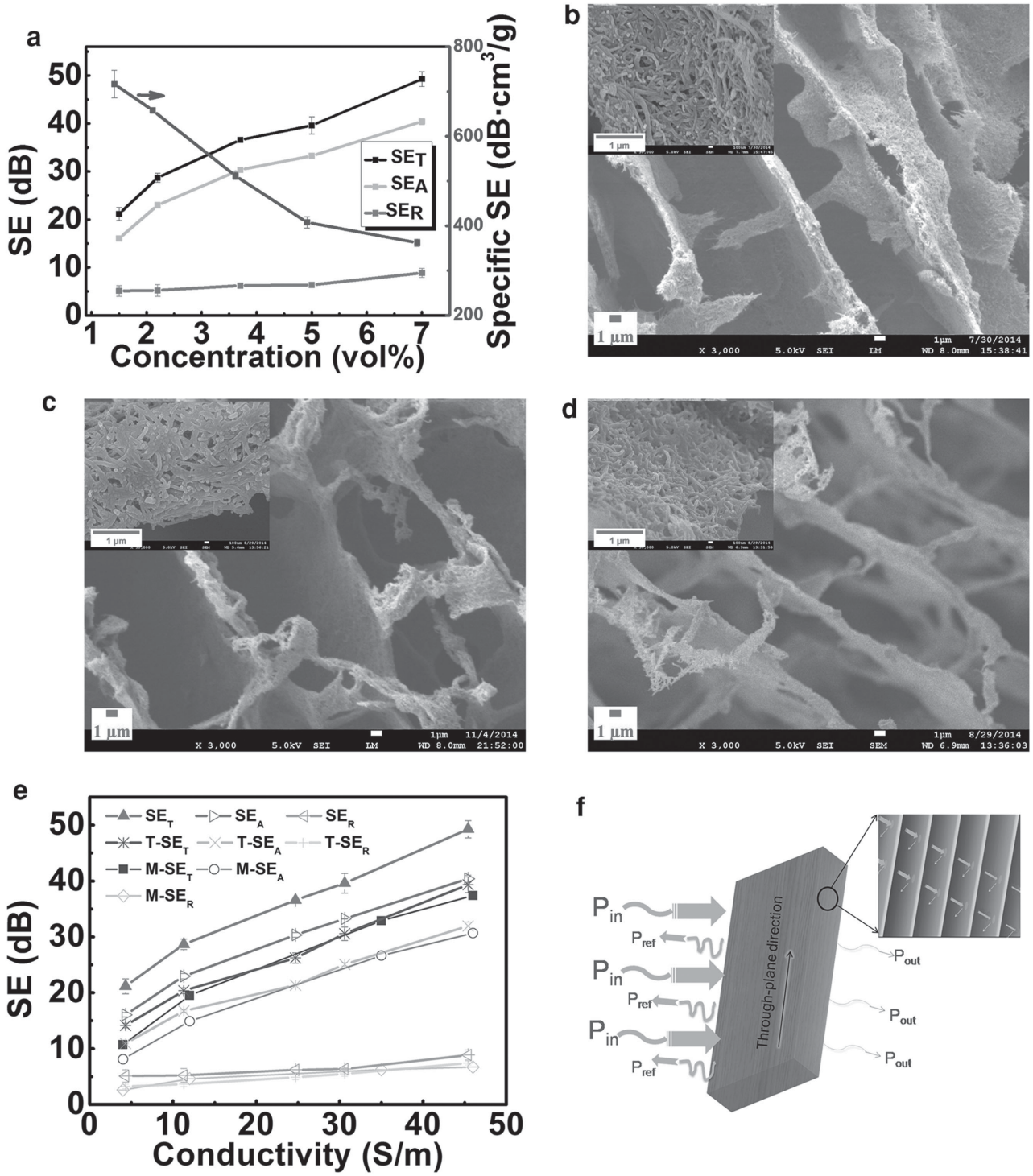

Figure 4. a) EMI shielding performance of 66.7 wt% MWCNT/WPU foams at frequency of 10 GHz as a function of MWCNT volume contents. Microstructures of 66.7 wt% MWCNT/WPU foams with various densities of b) 137, c) 72, and d) 29 mg cm^{-3}. e) EMI SE of theoretical predictions based on electrical conductivity and experimental values of 66.7 wt% MWCNT/WPU foams with various densities based on in-plane and through-plane directions at 10 GHz. f) Schematic representation of the shielding mechanism for the anisotropic porous composites in in-plane direction.

the multiple reflections of incident electromagnetic waves in the porous materials and thus enhance the SE_A and SE_T.[19,20,32] Combining those crucial arguments with our research, we consider that shape or orientation of the pores themselves in the porous shielding materials also plays a significant role in the shielding performance. Anisotropic porous structures of the porous MWCNT/WPU composites can introduce more interfaces in in-plane direction. As mentioned above, when the

incoming wave propagates along this direction, it interacts with more cell walls and is absorbed by means of the enhanced multireflection, leading to a far greater SE_A in the in-plane direction than that of the through-plane direction (Figure 4f). Combining with the high electromagnetic wave-absorbing ability of the cell walls derived from the synergic effect of high mass ratio of MWCNT and WPU, the porous composites in this study can indicate ultrahigh shielding performance in terms of SE and SSE.

3. Conclusion

Porous MWCNT/WPU composites with wide range of electrical nanofiller loadings are manufactured by a facile and low-cost freeze-drying method. The as-prepared composites are conducting and exhibit anisotropic porous structures, low densities, and excellent mechanical properties including flexibility. The lightweight conductive foams show very high EMI shielding performance in terms of SE (>50 dB in the X-band region) and SSE. The EMI SE can be controlled in wide range by effortlessly adjusting the fraction of electrical MWCNT, WPU matrix, and porosity. Densities of the porous MWCNT/WPU composites can reach as low as 20 mg cm^{-3} while SE is greater than 20 dB, corresponding to more than 98% weight reduction of the bulk composites; and thus high SSE (≈1148 dB cm^3 g^{-1}) that is higher than other shielding materials reported previously is obtained. Moreover, for the first time the shapes or orientations of the pores in the porous architectures are advised to optimize the EMI SE. The ultrahigh EMI shielding performance of our porous MWCNT/WPU composites can be ascribed to the high MWCNT mass ratios and conductivities of the cell walls, the interfacial polarizations of MWCNT and WPU, and the anisotropic porous structures. Combining the possibility of scalable manufacturing with easy-controllable feature, our porous composites show great potentials as lightweight, flexible, and ultrahigh performance shielding materials in academic and actual applications.

4. Experimental Section

Fabrication of Anisotropic Porous MWCNT/WPU Composites: MWCNT (TNM8, purity >95 wt%, average diameter ≈50 nm, and length 10–20 μm, supplied by Chengdu Institute of Organic Chemistry, Chinese Academy of Sciences (CAS)) aqueous solution (9 wt%) could be got by ultrasonic processing in 400 W for 15 min and mild magnetic stirring for 5 h with the aid of 1.5 wt% noncovalent surfactant (TNWDIS, aromatic modified polyethyleneglycol ether, supplied by Chengdu Institute of Organic Chemistry, CAS). The dispersion quality and stability of the CNT aqueous dispersion can be demonstrated by observing the UV–vis spectrum[33] (Figure S1d,e, Supporting Information). The porous composites containing various MWCNT contents were fabricated by magnetic stirring for 3 h of as-prepared MWCNTs dispersion and nonionic WPU emulsion (20 wt% solid content and ≈40 nm size of disperse phase particles), followed by freezing the mixed solution casted in mould with Teflon container and stainless steel bottom that is immersed in the liquid nitrogen, and freeze-drying the prepared hydrogels in the freeze-drying vessel (–50 °C and 20 Pa). In consideration of the cell walls of the porous composites are composed of MWCNT/WPU composites, the relevant solid MWCNT/WPU composite films are also prepared by casting the mixed solution onto the Teflon flat plate mould and drying at 70 °C for 5 h in the drying oven.

Characterization: The microstructure of the composites with various MWCNT contents was investigated by scanning electron microscopy (SEM, JEOL JSM-7500F). The resistance (R) of both porous the relevant solid composites were measured by four probe method with a Keithley 4200-SCS electrometer (Keithley, Cleveland, Ohio, USA) at room temperature. The electrical conductivity (σ) was obtained by the equation $\sigma = l/(R \cdot A)$, where A and l were the effective area and length of the measuring electrode, respectively. The compression behaviors in both directions of the porous samples were evaluated by a dynamic mechanical analysis (DMA, TA Q800), and at least five samples for each component of porous materials were tested. The samples with size of 22.86 mm × 10.16 mm × 2.3 mm were measured the EMI SE characterization in the frequency range of 8.2–12.4 GHz (X-band) within a waveguide method using a vector network analyzer (Agilent E8363B PNA-L), and more than five samples for each component were tested. The S-parameters of each sample were recorded and applied to calculate the EMI SE.

Supporting Information

Supporting Information is available from the Wiley Online Library or from the author.

Acknowledgements

This project was jointly supported by the National Key Basic Research Program of China (Grant Nos. 2012CB937503 and 2013CB934203) and the National Natural Science Foundation of China (Grant No. 11225210).

Received: August 25, 2015
Revised: September 25, 2015
Published online: November 20, 2015

[1] B. Wen, M. Cao, M. Lu, W. Cao, H. Shi, J. Liu, X. Wang, H. Jin, X. Fang, W. Wang, J. Yuan, *Adv. Mater.* **2014**, *26*, 3484.
[2] a) A. Namai, S. Sakurai, M. Nakajima, T. Suemoto, K. Matsumoto, M. Goto, S. Sasaki, S. Ohkoshi, *J. Amer. Chem. Soc.* **2009**, *131*, 1170; b) M. Arjmand, M. Mahmoodi, G. A. Gelves, S. Park, U. Sundararaj, *Carbon* **2011**, *49*, 3430.
[3] D. D. L. Chung, *Carbon* **2001**, *39*, 279.
[4] Y. Huang, N. Li, Y. Ma, F. Du, F. Li, X. He, X. Lin, H. Gao, Y. Chen, *Carbon* **2007**, *45*, 1614.
[5] B. Shen, W. Zhai, M. Tao, J. Ling, W. Zheng, *ACS Appl. Mater. Interfaces* **2013**, *5*, 11383.
[6] a) J. M. Thomassin, C. Jérôme, T. Pardoen, C. Bailly, I. Huynen, C. Detrembleur, *Mater. Sci. Eng., R* **2013**, *74*, 211; b) M. H. Al-Saleh, U. Sundararaj, *Carbon* **2009**, *47*, 2.
[7] M. Arjmand, T. Apperley, M. Okoniewski, U. Sundararaj, *Carbon* **2012**, *50*, 5126.
[8] Z. Chen, C. Xu, C. Ma, W. Ren, H. M. Cheng, *Adv. Mater.* **2013**, *25*, 1296.
[9] X. B. Xu, Z. M. Li, L. Shi, X. C. Bian, Z. D. Xiang, *Small* **2007**, *3*, 408.
[10] D. X. Yan, P. G. Ren, H. Pang, Q. Fu, M. B. Yang, Z. M. Li, *J. Mater. Chem.* **2012**, *22*, 18772.
[11] M. H. Al-Saleh, W. H. Saadeh, U. Sundararaj, *Carbon* **2013**, *60*, 146.
[12] a) M. Chen, L. Zhang, S. Duan, S. Jing, H. Jiang, M. Luo, C. Li, *Nanoscale* **2014**, *6*, 3796; b) A. Gupta, V. Choudhary, *Compos. Sci. Technol.* **2011**, *71*, 1563.
[13] a) M. C. Hermant, M. Verhulst, A. V. Kyrylyuk, B. Klumperman, C. E. Koning, *Compos. Sci. Technol.* **2009**, *69*, 656; b) V. Eswaraiah,

V. Sankaranarayanan, S. Ramaprabhu, *Macromol. Mater. Eng.* **2011**, *296*, 894; c) A. Ameli, P. U. Jung, C. B. Park, *Compos. Sci. Technol.* **2013**, *76*, 37.
[14] M. Antunes, M. Mudarra, J. I. Velasco, *Carbon* **2011**, *49*, 708.
[15] J. M. Thomassin, C. Pagnoulle, L. Bednarz, I. Huynen, R. Jerome, C. Detrembleur, *J. Mater. Chem.* **2008**, *18*, 792.
[16] Y. Yang, M. C. Gupta, K. L. Dudley, R. W. Lawrence, *Adv. Mater.* **2005**, *17*, 1999.
[17] Y. Yang, M. C. Gupta, K. L. Dudley, R. W. Lawrence, *Nano Lett.* **2005**, *5*, 2131.
[18] H. B. Zhang, Q. Yan, W. G. Zheng, Z. He, Z. Z. Yu, *ACS Appl. Mater. Interfaces* **2011**, *3*, 918.
[19] A. Ameli, P. U. Jung, C. B. Park, *Carbon* **2013**, *60*, 379.
[20] J. Ling, W. Zhai, W. Feng, B. Shen, J. Zhang, W. Zheng, *ACS Appl. Mater. Interfaces* **2013**, *5*, 2677.
[21] X. Shui, D. D. L. Chung, *J. Electron. Mater.* **1997**, *26*, 928.
[22] a) H. Zhang, I. Hussain, M. Brust, M. F. Butler, S. P. Rannard, A. I. Cooper, *Nat. Mater.* **2005**, *4*, 787; b) S. Deville, E. Saiz, R. K. Nalla, A. P. Tomsia, *Science* **2006**, *311*, 515; c) H. Zhang, A. I. Cooper, *Adv. Mater.* **2007**, *19*, 1529; d) Y. Tang, S. Gong, Y. Chen, L. W. Yap, W. Cheng, *ACS Nano* **2014**, *8*, 5707.
[23] H. Sun, Z. Xu, C. Gao, *Adv. Mater.* **2013**, *25*, 2554.
[24] J. Chen, H. Y. Liu, W. A. Weimer, M. D. Halls, D. H. Waldeck, G. C. Walker, *J. Am. Chem. Soc.* **2002**, *124*, 9034.
[25] a) S. T. Hsiao, C. C. Ma, W. H. Liao, Y. S. Wang, S. M. Li, Y. C. Huang, R. B. Yang, W. F. Liang, *ACS Appl. Mater. Interfaces* **2014**, *6*, 10667; b) S. T. Hsiao, C. C. M. Ma, H. W. Tien, W. H. Liao, Y. S. Wang, S. M. Li, Y. C. Huang, *Carbon* **2013**, *60*, 57; c) Z. Zeng, H. Jin, L. Zhang, H. Zhang, Z. Chen, F. Gao, Z. Zhang, *Carbon* **2015**, *84*, 327.
[26] a) M. Cadek, J. N. Coleman, V. Barron, K. Hedicke, W. J. Blau, *Appl. Phys. Lett.* **2002**, *81*, 5123; b) S. Cui, I. A. Kinloch, R. J. Young, L. Noé, M. Monthioux, *Adv. Mater.* **2009**, *21*, 3591; c) L. Gong, I. A. Kinloch, R. J. Young, I. Riaz, R. Jalil, K. S. Novoselov, *Adv. Mater.* **2010**, *22*, 2694.
[27] P. C. P. Watts, W. K. Hsu, A. Barnes, B. Chambers, *Adv. Mater.* **2003**, *15*, 600.
[28] K. Ji, H. Zhao, J. Zhang, J. Chen, Z. Dai, *Appl. Surf. Sci.* **2014**, *311*, 351.
[29] F. Moglie, D. Micheli, S. Laurenzi, M. Marchetti, V. Mariani Primiani, *Carbon* **2012**, *50*, 1972.
[30] M. H. Al-Saleh, U. Sundararaj, *Carbon* **2009**, *47*, 1738.
[31] B. Krause, G. H. Koops, N. F. A. van der Vegt, M. Wessling, M. Wübbenhorst, J. van Turnhout, *Adv. Mater.* **2002**, *14*, 1041.
[32] J. Wang, C. Xiang, Q. Liu, Y. Pan, J. Guo, *Adv. Funct. Mater.* **2008**, *18*, 2995.
[33] a) A. H. Korayem, M. R. Barati, G. P. Simon, T. Williams, X. Z. Zhao, P. Stroeve, W. H. Duan, *Langmuir* **2014**, *30*, 10035; b) J. Yu, N. Grossiord, C. E. Koning, J. Loos, *Carbon* **2007**, *45*, 618.